Quantifying small-scale deforestation and forest degradation in African woodlands using radar imagery

Quantifying small-scale deforestation and forest degradation in African woodlands using radar imagery

Casey M Ryan[1], Timothy Hill[1,2], Emily Woollen[1], Claire Ghee[1,3], Edward Mitchard[1], Gemma Cassells[1], John Grace[1,2], Iain H Woodhouse[1] and Mathew Williams[1,2]

1. School of Geosciences, University of Edinburgh, EH9 3JN.

2. The National Centre for Earth Observation, Natural Environment Research Council, UK.

3. Now at: The James Hutton Institute, Invergowrie, Dundee DD2 5DA.

Corresponding Author:

Casey Ryan, tel: +44 131 650 7722 casey.ryan@ed.ac.uk

Key words: carbon mapping, emissions, land use change, agriculture, machamba, carbon stocks, ALOS PALSAR, radar, backscatter

Word count: 7102

Running title: Quantifying forest loss in African woodlands

Abstract

Carbon emissions from tropical land use change are a major uncertainty in the global carbon cycle. In African woodlands, small-scale farming and the need for fuel are thought to be reducing vegetation carbon stocks, but quantification of theseprocesses is hindered by the limitations of optical remote sensing and a lack of ground data.

Here we present a method for mapping vegetation carbon stocks and theirchanges over a three year period in a >1000 km^2 region in central Mozambique at 0.06 ha resolution. L-band synthetic aperture radar imagery and an inventory of 96 plots are combined using regression and bootstrapping to generate biomass maps with known uncertainties. The resultant maps have sufficient accuracy to be capable of detecting changes in forest carbon stocksof as little as 12 MgC ha^{-1} over 3 years with 95% confidence. This allows characterisation of biomass loss from deforestation and forest degradationat a new level of detail.

Total aboveground biomass in the study area was reduced by 6.9±4.6% over three years: from2.13±0.12 TgC in 2007 to 1.98±0.11 TgC in 2010, a loss of 0.15±0.10 TgC. Degradation probably contributed 67% (96.9±91.0 GgC) of the net loss of biomass, but is associated with highuncertainty.

The detailed mapping of carbon stock changes quantifies the nature of small-scale farming. New clearances were on average small (median 0.2 ha) and were often additions to already cleared land. Deforestation events reduced biomass from 33.5 to 11.9 MgC ha^{-1}on average. Contrary to expectations, we did not find evidence that clearances were targeted towards areas of high biomass.

Our method is scalableand suitable for monitoring land cover change and vegetation carbon stocks in woodland ecosystems, and can support policy approaches towards reducing emissions from deforestation and degradation (REDD).

Introduction

Deforestation and other land use change is a major component of the anthropogenic carbon (C) cycle, transferring 0.9-2.2 PgC $year^{-1}$ from the biota to the atmosphere (Houghton, 2010).This number is highly uncertain (Denman *et al.*, 2007, Ramankutty *et al.*, 2007, van der Werf *et al.*, 2009, Houghton, 2010) and estimates often exclude many of the processes leading to degradation of forest land (Houghton, 2010). Deforestation is primarily the result of the clearing of land for agriculture (Geist & Lambin, 2002), both for the large-scale production of global commodities (DeFries *et al.*, 2010), and, particularly in Africa, for small-scale production of food and cash crops (Burgess *et al.*, 2002, Fisher, 2010).In Africa, land use changeemissions are thought to be in region of 0.3 ± 0.2 PgC $year^{-1}$(Houghton & Hackler, 2006, Williams *et al.*, 2007, Ciais *et al.*, in press), but the data underlying these estimates come from extrapolation of outdated, unreliable and inconsistent national estimates (Grainger, 2008, Kindermann *et al.*, 2008, FAO, 2010).

Woodlands, characterised by an open tree canopy and a continuous grass layer, cover 36% of vegetated Africa (Mayaux *et al.*, 2004), and as such represent a low density, but large, stock of vegetation C(Dewees *et al.*, 2010). African countries dominated by woodlands have high population densities, high population growth rates and high, but uncertain,deforestation rates (FAO, 2010). As a result, nations dominated by woodlands contribute around half of Africa'sdeforestation emissions (based on data from Mayaux et al. (2004) and FAO(2010)). Woodlands are particularly difficult to monitor with optical/infraredremote sensing due to inter- and intra- annual changes in tree leaf display (Grainger, 1999)and the transient presence of a substantial grass layer which complicates the interpretation of such satellite imagery (Archibald & Scholes, 2007). Consequently, degradation emissions from woodlands are highly uncertain, but are thought to be substantial (Ahrends *et al.*, 2010).

The standard approach to estimating C emissions from deforestation is based on estimates of changes in forest area, aided by increasingly robust estimates of forest area change (Etter *et al.*, 2006, Achard *et al.*, 2007, Hansen *et al.*, 2008, Miettinen *et al.*, 2011). Degradation emission estimates however, require repeat *in situ* measurements of carbon density (GOFC-GOLD, 2010) which are scarce(Ahrends *et al.*, 2010), because they require a large number of plots and strata to estimate accurately any changes in mean C density. Recent airborne approaches (Asner *et al.*, 2010)have not been widely deployed to date.As a result, changes in forest C density resulting from fire (Ryan & Williams, 2011) or the selective extraction of biomass for fuel or timber (Nepstad *et al.*, 1999), are rarely assessed and have not been fully included in emissions estimates (Houghton & Hackler, 2006, Denman *et al.*, 2007).

Even when combined, the methods outlined above yield large uncertainties on estimates of changes in vegetation C stock, let alone on emissions(Houghton *et al.*, 2009).Uncertainty stems from three main issues: 1)The use of arbitraryforest/non-forest thresholds whereasC stocks are a continuous variable. Such thresholds are a particular problem in woodlands where distinct edges are rare; 2) a lack of *in situ* measurements of C density,and the potential artefacts associated with differential land use on research plots; and 3);land that is deforested or degraded may not be representative of the forest type in which it is found (Loarie *et al.*, 2009, Houghton, 2010).That is, farmers are likely to target areas for deforestation based on careful consideration of agricultural potential. Therefore, land with higher than average soil fertility and/or water availability might be expected to have a greater probability of conversion to agriculture. The same areas might also be expected to have higher than average soil and vegetation C stocks due to the increased productivity.

Small scale, often shifting, cultivation exemplifies the problem of estimating changes in C stocks in forests and woodlands,producing a mosaic landscape that is frequently misclassified (Mertz, 2009) and is rarely well-represented by discrete land cover classes. The landscape C dynamics (Williams *et al.*, 2008)cannot be adequately described by changes between

categories such as degraded land, forest or agriculture (Schmidt-Vogt *et al.*, 2009). Furthermore, the scale at which small-scale farmers clear forest is constrained by a lack of mechanical power and transport. This physical limit results in small farms (scale ~ha) that may not be recorded on land use maps or detected with accuracy by coarse-scale (~km^2) satellite-based landcover change analyses.

Thus, there is a clear need for direct measurement at sub-hectare resolution of changes in C stocks due to land cover change (Houghton *et al.*, 2009). Our first aim is to demonstrate a method for such measurements in African woodlands at a spatial resolution sufficient to characterisesmall scalefarming and degradation. This is achieved by the use of 25 m resolution L-band radar imagery to map C stocks and their changes through the years 2007-10 in an area of central Mozambique. Radar imagery has several advantages for this purpose. Firstly, cloud and atmospheric effects are largely irrelevant allowing observations at cloudy sites. Secondly, L-band (23 cm wavelength)normalised radar cross section (hereafter referred to as backscatter)has been shown to have a reasonably direct relationship to woody biomass up to a saturation at around 50 MgC ha^{-1}(Le Toan *et al.*, 1992, Rignot *et al.*, 1994, Magnusson *et al.*, 2007, Karjalainen *et al.*, 2009). These advantages mean that spaceborneradar imagery is increasingly used in support of land use mapping in the tropics (van der Sanden & Hoekman, 1999, Hoekman *et al.*, 2010, Rahman & Sumantyo, 2010). Previous work has shown that L-band radar backscatteris well-correlated to biomass across several African landscapes (Mitchard *et al.*, 2009).

The resultant C maps allow us to ask several questions about the nature of the processes of deforestation and degradation:

- How much carbon is lost to deforestation compared to degradation?
- Are areas of high carbon density preferentially targeted for land cover change?
- What is the carbon density of changed areas before and after land cover change?

- What size are land cover change events, and how are they clustered in space?

Methods

Site description and land use history

Our study areacovers 1,160 km^2 in the Gorongosa and Nhamatandadistricts of Sofala province in central Mozambique. It is primarily dominated by miombo woodland, the most widespread vegetation type in Southern Africa (Frost, 1996). It has a seasonal wet-dry climate with ~900 mm rain per year, with 82% falling in the five months between November and March(Ryan *et al.*, 2011). The vegetation consists of miombo woodland on the well-drained flanks of the Rift valley, grading to more scattered savanna on the poorly drained valley floor (Tinley, 1977, 1982). The terrain is gently undulating in most of the study area, but in the west there are steep slopes associated with the Pungue and Vunduzi rivers (Fig S1). Ninety seven per cent of the study area has a slope of < 10°(based on 90m resolutionelevation data from the Shuttle Radar Topography Mission (SRTM, Farr *et al.*, 2007, http://srtm.usgs.gov).

The area is undergoing rapid land use change: in 1992, with the end of the Mozambican civil war, there were major population movements in the area, including resettlement of semi-abandoned rural areas such as Nhambita (Fig 1). The only surfaced road in the area, the EN1, was rebuilt, along with a bridge over the River Pungue (rehabilitation of both took place from 1999-2002), connecting the study area and Gorongosa town to the Beira corridor, the major area of economic activity in central Mozambique. Gorongosa town has grown rapidly since 1992 (INE, 2010) with the district population increasing by 50% from 1997 to 2007 to 117,129. Currently, 69% of the population is aged below 18 years(INE, 2010). Forest or woodland loss in the area is primarily the result of: 1) clearance for small scale agriculture, notably for maize production on farms of between ~1-2 ha and 2) charcoal production, involving the selective removal of medium size stems from an area of ~0.2 ha surrounding

temporary kilns. Charcoal is sold along the EN1 highway for transport south to Inchope and Beira, but there is also some demand for charcoal and fuel wood in Gorongosa town. In addition, fire is extensively used to manage the landscape and wild fires are common. Frequent and intense fires can reduce biomass in these woodlands (Furley *et al.*, 2008, Ryan & Williams, 2011).

Carbon stock estimation

The basis of our approach is to produce a three year time series of carbon maps of the area. The maps are produced using a combination of satellite radar imagesand *in situ* carbon stock inventories. We deal here only with carbon in the aboveground woody vegetation pool (AGB, MgC ha^{-1}), although more information on belowground biomass at this site can be found in Ryan et al (2011).

Radar imagery

Synthetic Aperture Radar (SAR) remote sensing can provide information on vegetation biomass (Le Toan *et al.*, 1992), as well as many other characteristics of the land surface (Woodhouse, 2006a). SAR utilises an active sensor aboard a satellite or plane to send out a beam of energy and measures the intensity of the echoes that return to the sensor. The parameter of interest is the *backscatter* (technically the normalised radar cross-section, a unitless variable (m^2/m^2)). Backscatter can loosely be thought of as the ratio of the power that comes back from a patch of ground to the power sent to that patch of ground (based on the arbitrary assumption that the ground is an isotropic scatterer). The energy that returns to the sensor varies with the proportion of the incident energy that is scattered by the land surface, and the directionality of that scattering. When energy of an appropriate wavelength is used, it interacts with the structural elements of the tree canopy (branches and trunks): typically, more woody biomass results in more diffuse scattering and thus more energy being returned to the sensor and a higher backscatter value is recorded. Backscatter is also affected by soil

roughness (as it changes the directionality of the scattering) and moisture (as it changes the total proportion of scattering), as well as other environmental factors. In this study L-band (~23 cm wavelength) SAR imagery was used, as it is less affected by soil conditions than shorter wavelengths, and is known to be able to detect deforestation and to be sensitive to forest biomass due to its ability to penetrate the forest canopy (Almeida-Filho *et al.*, 2005, Fransson *et al.*, 2007, Karjalainen *et al.*, 2009, Mitchard *et al.*, 2009). Ten images were acquired that covered the study site spanning the dates 23 Jun 2007 to 1 Oct 2010 (Table 1). All images were for the dry season and two or three were available for each year.

The technical details of the imagery and processing now follow. Images were obtained from the Phased Array L-band Synthetic Aperture Radar sensor aboard the Advanced Land Observing Satellite (ALOS PALSAR) in the Fine-Beam Double mode (Shimada *et al.*, 2010). All images were acquired on the ascending pass, have an incidence angle centred on 34.3°, and were provided at a pixel size of 12.5m with 4 equivalent looks, but then averaged to 25 m for 16 equivalent looks. Only Horizontal-send Vertical-receive data are used here, as previous studies have shown this polarisation to be more sensitive to biomass than Horizontal-send Horizontal-receive (Le Toan *et al.*, 1992, Mitchard *et al.*, 2009).

The images were processed using the Alaska Satellite Facility's MapReady software v2.3.6 (ASF, 2010), combined with ~90 m elevation data from the SRTM. Each image was converted from digital numbers to backscatter using the calibration coefficients of Shimada *et al.*(2010) and a geometric and radiometric terrain correction was applied.Visual comparison with optical imagery (IKONOS and Landsat) showed that the resulting images were well geolocated (1-2 pixel error, i.e. 25 -50 m) compared to prominent landscape features such as roads, bridges and an airstrip. In particular, the images were very closely geolocated to each other: no geolocation differences were visible between the ten images. Commonly,backscatter values are used on the logarithmic dB scale, but here untransformed values of backscatter are

used,as the backscatter-biomass trendis usually linear in untransformed space, but non-linear in dB space.

Ground data

For each radar scene, backscatter values were converted into carbon density using a regression equation based on inventories of 96 plots in the forest, woodland and cropland in the south of the study area. These data come from a range of inventories conducted during 2006-9, and include plots of sizes ranging from 0.1 to 2.2 ha (mean±SD 0.63±0.33 ha, Fig2). The inventories include standing trees > 5 cm DBH. Many of the woodland inventory data are described in Ryan *et al*. (2011), as is the site-specific allometric equation for converting stem diameter to carbon mass for each stem. Briefly, the data set consist of: fifteen 1 ha square permanent sample plots in the woodland and savanna (Ryan *et al.*, 2011), eight 0.28 ha plots used in the fire experiments of Ryan and Williams (2011), thirty 0.57 ha plots in a transect from open savanna to woodland (Woollen et al. in prep; these had a nested sampling design, see supplementary information), five 0.5 ha plots in relatively remote woodland, thirty-seven plots of 0.1 to 2.2 ha (mean 0.6 ha) on cropland (Ghee, 2009) and one dense forest plot consisting of three 0.04 ha subplots. Details of the plot data are given in the supplementary information. Every plot is thought to have avoided abrupt land cover change (i.e. deforestation) during the study period, assessed by repeat ground visits or satellite imagery; however we cannot rule out gradual changes due to aggradation or degradation.

Regression and Error Propagation

To convert backscatter images into aboveground biomass (AGB in units of MgC ha^{-1}), for each timeslice we regress plot mean backscatteragainst plot AGB, assuming that the plot AGB is consistent over the observational period. We use reduced major axis (RMA) regression (Mitchard2011, in review) implemented in MATLABby Trujillo-Ortiz & Hernandez-Walls (2010). RMA regression minimises the errors on both axes (rather than just

on the Y-axis as in normal regression), which is appropriate because there are errors in both data sets and the observer controls neither (Sokal & Rohlf, 1995).

To estimate error on the predictions from the regression, a 5,000 x 2-fold cross-validation procedure was employed. Half the dataset was withheld and used to estimate the root mean squared validation error (RMSE), and bias (B) of predictions from each regression. These statistics are defined as (Hui & Jackson, 2007):

$$\mathrm{B} = \frac{\sum_i Y_i - \hat{Y}_i}{n}$$

$$\mathrm{RMSE} = \sqrt{\frac{\sum_i (Y_i - \hat{Y}_i)^2}{n-2}}$$

Where Y_i is a validation data point (not used in the regression) and $\hat{Y}_i$ is the prediction from the regression. B and RMSE were calculated for all 10 timeslices5,000 times, each time with a different random split of the data, and the mean values of B and RMSE for the 5,000 validations are reported. For indicative purposes the adjusted R^2 of an ordinary least squares regression is also shown in Table 1.

The temporal covariance of the bias was quantified by looking at the correlation of the bias between time steps for each of the 5,000 validations, i.e. by asking if the regression is biased high in year *x*, is it likely to be biased high in subsequent years *x*+*n*?

Regression errors were propagated to the carbon maps with a bootstrap procedure. Bootstrapping was used as it implicitly includes any spatial or temporal covariance of the uncertainty resulting from the AGB-backscatterregressions. For each set of 10carbon maps, 30,000 realisations were created each using a different regression based on randomly selected regression data (resampled with replacement). Derived quantities such as carbon stock change, rates of loss, and the deforestation and degradation totals, were also calculated for each of the 30,000 bootstraps, allowing the uncertainties introduced by the regression to be estimated. All values are reported as the mean ± the standard deviation of the 30,000

bootstraps. The number of bootstraps was chosen after initial analysis showed that repeat calculation with different random number seeds using 10,000 bootstraps yielded identical results to three significant figures.

Change detection algorithm

One of the aims of this paper is to estimate parameters of pixels before and after land cover change. This necessarily involves defining a threshold of change. Here we focus on detecting abrupt losses of AGB and define land cover changes (LCC) of interest as being in pixels where: 1) AGB is >20 MgC ha^{-1} at the start of the study, thus increasing the likelihood that only forested pixels are examined; 2) the AGB of the pixel after the change is reduced to a minimum percentage (φ, default 50%) of its initial AGB, a threshold which should exclude most natural changes in forest structure; and 3) the probability that the change in AGB occurred by chance (given the noise in the data) is $<(1-\alpha)$ (default $\alpha = 0.95$). The use of a ratio to define change is appropriate with SAR imagery in power space, as ratioing SAR images is generally preferred to differencing because of its noise characteristics (Rignot & van Zyl, 1993, Radke *et al.*, 2005).

The time series $C(t)$, where C is the AGB of a pixel over the t=1,…,10 images, provides a rich data source with which to detect changes, and the 10 time-slicesallow more confidence in using noisy data. For change detection, a simple iterative algorithm locates the time-point of change, τ, at which the mean of the preceding values of $C(t)$ is most different to the mean of the remaining part of the time series. The mean AGB before ($C1$) and after ($C2$) τ are then estimated. We use a Monte Carlo procedure to estimate the probability, P, of obtaining the change in AGB ($C1$-$C2$) by chance, based on sampling from the time series and including the RMSE validation errors from the regression (Table 1). A mathematical description is given in the supplementary information.

Once changed pixels have been identified, each LCC event (defined as adjacent changed pixels that have identical τ) was automatically converted to a polygon in ARCGIS (ESRI, CA, USA)and the area of each polygon calculated.

Change detection validation

Two tests were used to produce accuracy statistics for the change detection. To assess successful LCC detection we delineated 92 agricultural fields formed by clearing woodland between March 2007 and June 2009. These conversions were assessed by visual interpretation of multispectral SPOT 4 (20 m resolution) imagery from 7 March 2007 and IKONOS (1 m) imagery from 24 June 2009 (an example is shown in Fig6). The edges of the new farms were converted by hand to polygons using ARCGIS. These areas of known LCC had a mean area of 1.7±1.5 ha and were well distributed across the study area. Although the AGB of these new farms is unknown, visual inspection suggests that very few trees remain and that they have crossed the change threshold outlined above. The miss rate is defined as the number of pixels on these farms that are not detected as changed.

To assess false positives, an area of the Gorongosa National Park, termed 'The Sanctuary' (Fig1) that is extremely unlikely to have undergone human-induced LCC was analysed. The Sanctuary is an electric-fenced area of 5,761 ha designed to retain animals imported to the Park (not including elephants). Note that this definition of false positive is very broad and includes both natural changes to the woodland as well as random errors in detection as 'false positives'.

The sensitivity of the hit rate and false positive rate to the parameters used in the change detection algorithm was assessed: φ, the fraction of AGB remaining on a changed pixel was varied from 80% to 20%, and α, the threshold *P*-value above which a LCC event is considered significant, from 0.8 to 1.

Assessing preferential selection of high biomass areas

To test whether land with high AGB is preferentially selected for LCC, compared with the null hypothesis that LCC is random with respect to AGB, we compare the observed results to a pseudo-data set for which the null hypothesis is true. The pseudo data time series of AGB for each pixel, denoted *C*(t)*, is constructed as follows: for each pixel, a time series is constructed with a constant mean equal to the observed AGB in 2007. Then a random 4% of pixels are pseudo deforested at a time point randomly selected between *t*=2 and *t*=9. At this time point, an abrupt change is imposed and the AGB reduced to a mean of 10 MgC ha^{-1}. Noise was added to the time series by drawing each value from a normal distribution with means as described above and standard deviations *N(t)*, the RMSE validation errors from the regressions. The change detection algorithm was run as described above to identify pixels that were pseudo-changed, estimating the parameters *C1** and*C2**, the pseudo equivalents of *C1* and *C2*. The resulting distributions of *C1**and*C1* are compared using a two sample Kolmogorov-Smirnov test to test if the distribution of *C1* is larger than *C1**.

Biomass lossdue to deforestation and degradation

To compare the contributions of deforestation and degradation to the total carbon loss from the study area, the change (ΔC) between the mean AGB of the three images in 2007 (C_{2007}) and the mean AGB of the three images in 2010 (C_{2010}) was examined. The image is classified into four categories that follow the conventional definition of de/reforestation and de/aggradation based on a binary forest/non-forest pixel classification in 2007 and 2010. The forest/non-forest classification is made using a default AGB thresholdof 15 MgC ha^{-1}. However, the effects of varying the threshold from 5 to 20 MgC ha^{-1} were evaluated.

The deforestation AGB loss (Δ_D) is defined as the net sum of ΔC for pixels that shift from the forest to non-forest classes. Reforestation gain (Δ_R) is the net sum of ΔC for pixels moving from non-forest to forest. Forest de/aggradation (Δ_{GF}) is the net sum of ΔC for forest-pixels

remaining forest, and non-forest de/aggradation (Δ_{GN}) is the net sum of ΔC for non-forest pixels remaining non-forest. Thus:

$$C_{2007} - C_{2010} = \Delta C = \Delta_D + \Delta_R + \Delta_{GF} + \Delta_{GN}$$

and net deforestation is:

$$\Delta_{D,net} = \Delta_D + \Delta_R$$

Thus for all terms describing a change in biomass stocks, positive numbers indicate loss of biomass and negative values denote gains.

Results

Ground data and regression

The 96 plots ranged in aboveground biomass from 0 to 56 MgC ha^{-1} (mean 15±12 MgC ha^{-1}; Fig 2; ± indicates one standard deviation throughout). The ordinary least squares regression of backscatter against AGB gave values of R^2 from 0.40 to 0.58 (Table 1). For the ten images, regression slopes ranged from 1272 to 1803 (MgC ha^{-1})$^{-1}$ (Table 1; Fig3) and this translated into moderate variation in estimated carbon stocks through the study period. For instance,backscatter values for a pixel over a pseudo invariant patch of protected forest ranged from 89-107% of the first image, which translated, to a range of 47-61 MgC ha^{-1} (Fig 4).

The validation procedure estimated RMSE validation errors of 8.7 – 10.9 MgC ha^{-1} for the different time slices (mean error 9.8±0.7 MgC ha^{-1}), and mean absolute bias of 1.6±0.1 MgC ha^{-1} (Table 1). The worst-case scenario for change detection is that these biases are random between each scene, but the covariance of these biases through time was high(Table S1), with, for example r>0.86 between the bias in the three scenes from 2007, and r>0.44 for bias between years.

Carbon stocks and changes

The carbon stocks in the study area exhibit an east-west gradient related to the topography, with AGB ~60 MgC ha^{-1} in the undisturbed areas to the west of the Vunduzi river falling to ~30 MgC ha^{-1} in the centre of the study area (Fig 1). East, towards the floor of the Rift valley, substantial biomass is restricted to the river lines and high points. Imposed on this topographic pattern, the effects of human disturbance are obvious, with almost no large blocks of woodland remaining to the south of the River Pungue and along the west side of the highway. However LCC is less apparent to the east of the highway, an area that is part of the buffer zone of the Gorongosa National Park. The town of Gorongosa marks the epicentre of a zone of reduced biomass.

The study area contained AGB of 2.13±0.12 TgC in 2007 and 1.98±0.11 TgC in 2010, a loss of 0.15±0.10 TgC, or 6.9±4.6% of the 2007 AGB over three years. Pixels that lost > 9 tC/ha contributed half the total loss in AGB, with the remaining loss being in pixels that lost <9 tC.

Spatial patterns of carbon stock change

Looking at the spatial patterns of change in C stocks (Fig 5), there were several areas of increasing AGB mainly in the Park and Sanctuary (A; letters refer to points marked on Fig 5; names to the sub-areas delineated with green lines in Fig 1) as well as decreases (B). Losses were observed all along the highway, but particularly to the west of the road; in comparison, to the east of the road in the buffer zone of the Park there are fewer areas of biomass loss (C). New farms were opened in the area between the Vunduzi river and the road, and a cluster of new farms can be seen in the inaccessible region to the west of the river (D). A new power line built in the Park is visible along the boundary of the Nhambita sub area (E). An area of private land, in which charcoal production and agriculture are not present (Eng. A. Serra, pers comm. 2011) stands out clearly from the surrounding decrease in AGB in Mbulawa(F). In Nhambita a string of new farms along a previously high AGB river line is visible (G).

The probability distribution functions (PDFs) of carbon stocks in the sub areas (Fig 7) provide further insight into the AGB stocks and changes. In the inhabited areas (Gorongosa town, Nhambita, Mucombeze and Mbulawa) the LCC is evident in the difference between the 2007 and 2010 PDFs. In contrast, in the Sanctuary, the 2010 PDF is shifted to higher biomass values compared to 2007, indicating regrowth. The Remote Park shows no change in AGB over the study period. Vunduzi, an almost undisturbed, well wooded area, is the only sub-area with a normal PDF. The bimodal PDF of Gorongosa appears to consist of a deforested PDF similar to Mucombeze combined with a woodland PDF centred on 40 MgC ha^{-1}.

Deforestation and degradation

The loss of AGB across the study area over the three years was 149±101GgC. Using the default threshold of forest being any pixel with AGB > 15 MgC ha^{-1}, loss of AGB due to deforestation was 92±11GgC (Table 2). This was offset by a reforestation gain in AGB of -36±4.5GgC, leading to a net deforestation loss of 55±12GgC. This can be compared to forest degradation loss of 42±73 GgC and non-forest degradation of 53±43GgC, so that total degradation is 94±90 GgC. Thus most of the uncertainty in ΔC comes from the degradation term.

Thus, the best guess of the percentage of net biomass lossthat can be attributed to degradation is 67% (median of the bootstraps). This result varied only slightly with different thresholds of forest/non-forest: from 69% with 10 MgC ha^{-1}as the threshold to 65% when using 20 MgC ha^{-1} as the threshold. This proportion of biomass loss attributed to degradation is highly uncertain, with an 80% confidence interval of 21 to 80% (Fig S2). There is a 79% chance that degradation was >50% of the net loss of AGB and a 90% chance that it accounted for >21% of the net loss.

Characteristics of land cover change events

The change detection algorithm was able to detect per-pixel abrupt changes of >12 MgC ha^{-1}, a threshold that is a function of the noise associated with the measurements of AGB, the number of observations and the detection algorithm parameters α and φ. Using the default parameters (α = 0.95 and φ = 50%) abrupt LCC was detected in 2.61 % of the study area.

In total, 3,029 ha were detected as changed in 6,761 events (mean size = 0.45±0.80 ha, median = 0.19 ha). Events larger than the median contributed 88% of the total changed area; events > 0.5 ha, 70%; and events >1 ha contributed 49% of the total changed area. The mean event size (assumed to be false positives) in the Sanctuary (0.14 ha) was smaller than the events in the inhabited sub-areas (means 0.34-0.52 ha). In the inhabited areas, event size was smallest in Mucombeze (mean 0.34 ha), where forested land is very scarce (26% of land was forested in 2007) and largest (mean 0.52 ha) in Vunduzi where all land was forested in 2007. The other inhabited sub-areas have intermediate event sizes and forest cover.

The mean change is AGB when an event occurred was for the area to lose 21.3±5.5 MgC ha^{-1}, being reduced from *C1* = 33.5±9.8 to *C2* = 11.9±18.4 MgC ha^{-1}. The reduction in AGB ranged from 12.2-56.9 MgC ha^{-1}. With the exception of the Vunduzi sub-area, the mean pre-change AGB of changed pixels (*C1*) was never more than 0.7 MgC ha^{-1} higher than if LCC was random with respect to AGB (*C1**), although the differences were significant to P<0.001 (Fig7). This suggests that the hypothesis that high AGB pixels are preferentially subject to LCC is not true to a substantial extent. However, in the Vunduzi sub-area, *C1* (53.6 MgC ha^{-1}) was 4.7 MgC ha^{-1} higher (P<0.001) than *C1** (48.9 MgC ha^{-1}), suggesting a modest preference towards high AGB land, but the number of changed pixels is relatively small (n= 345).

Events were significantly clustered (P<0.001) according to the nearest neighbour distance. The observed mean distance from one event to the nearest was 87 m compared to 206 m if the

events were evenly spaced. Many cleared areas are the result of small expansions to the frontiers of already cleared land (example in Fig 6).

Change detection validation and sensitivity

Using our default parameters, LCC was detected in 1,646 of the 2,611 validation pixels, a miss rate of 35%. Generally, the missed pixels were at the fringes of the events – only in 10 of the 90 validation events was no LCC detected – implying that the misses will affect the size of detected events more than the number. The false positive rate was 0.016% in the Sanctuary, equal to 0.005 % year^{-1}. The sensitivity analysis (Fig 8) showed that it is possible to suppress the false positive rate further, but only at the expense of an increase to the miss rate. A zero false positive rate can be achieved in the Sanctuary by reducing φ to 20% (for $\alpha > 0.95$), but this gives a miss rate of 74%. Conversely, a lower miss rate can be achieved, say 20%, with φ =60% and α=0.9, but this gives a false positive rate of 0.07%.

Discussion

Can L-band radar accurately measure changes in biomass?

Our method was able to detect a loss (6.9±4.6%) of biomass from the landscape over a relatively short observation period of three years. This change in biomass (ΔC) is equivalent to a reduction in C density from 18.4 to 17.1 MgC ha^{-1} across the whole study area, a change that would be difficult to detect without very accurate stratification and intensive ground-based sampling. The relative error on the standing stock estimates is 6%, but this increases to 67% for ΔC,the change in stocks(Table 2). Without the high covariance of the regression errors through time (Table S1) the error on the change in stocks would have been higher.

If the net changes in biomass are split between deforestation and degradation, it is clear that most of the uncertainty in ΔC comes from degradation. It is much easier to detect change in the small area (77 km^2) that was deforested and which lost 84.8±9.7 GgC, compared to the

very large (643 km^2) forest-remaining-forest area that probably lost a comparable amount of AGB (96.9±91.0 GgC)(Table 2). The nature of the challenge is illustrated by a best guess assessment of the change in C density for the forest-remaining-forest area from 30.3 to 29.4 MgC ha^{-1}.

However, at a pixel scale, abrupt change (including degradation) is detectable at 95% confidence as long as it exceeds 12 MgC ha^{-1}. Per pixel change detection rates were 65%, and in 89% of change events some change was detected. These rates are comparable to another application of L-band SAR to detect >2 ha clear cuts in Sweden (hit rate = 76%, (Pantze *et al.*, 2009)). However it is clear that we are at the limit of the resolution of this technique – the ALOS imagery detects new farms as having a bare centre and then a gradient of biomass into the surrounding woodland, but on-the-ground observations show that the farm/woodland boundary is normally abrupt. Morphological detection techniques have the potential to improve the very simple per-pixel change detection used here and to reduce false positives. Such techniques may also be more accurate in determining the size of each LCC event.

Backscatter-biomass relationships for space borne L-band backscatter in 'difficult' conditions (i.e. mixed age stands of multiple species) are reported with similar statistics to that found here (e.g. R^2 = 0.53 (Karjalainen *et al.*, 2009)) and slightly better results have been found in even-aged stands (RMSE = 30% of biomass (Magnusson *et al.*, 2007)), or when considering a very wide range of biomass (Mitchard *et al.*, 2009). In comparison, airborne LiDAR has regression statistics between the LiDAR metrics and AGB of RMSE of 23.5 MgC ha^{-1}, R^2 = 0.85 in an example from Peru (Asner *et al.*, 2010). In the present study the comparable figures were RMSE = 8.7 tC/h and R^2 = 0.49, but the difference in RMSE is probably due to the lower AGB of our study area.

Williams et al (2008) found that regrowing woodland at this site can accumulate between 0.4-0.9 MgC ha^{-1} $year^{-1}$ AGB, and we expect that changes in more mature woodland will be less than this. However, in two parts of the study area (Fig 5, A) rapid increases in AGB beyond

this rate are observed. Observations in this area show rapid woody encroachment, probably the result of fire exclusion in the Sanctuary. Stem numbers have approximately doubled in four years (data not shown), but biomass has not increased by that rate because the new stems are small saplings. This unrealistic sensing of biomass accumulation raises the issue of which (combination of) plot characteristics L-band backscatter is most strongly related to – stem number, basal area or biomass (Woodhouse, 2006b)? In mixed age, diverse sites this question has not yet been resolved (Woodhouse, 2006b). If the biomass-backscatter relationship is not direct, but is mediated by other stand characteristics(Lucas *et al.*, 2010), then the site-specificity of the regression parameters needs to be evaluated (Mitchard *et al.*, 2009).

- How much carbon is lost to deforestation compared to degradation?

The large uncertainty on the degradation loss makes it difficult to estimate the fraction of AGB losses attributable to degradation. However, a best guess is that total degradation was 67% of total net losses of AGB. This analysis thus provides tentative support for the idea of a large and presently un-quantified loss of biomass due to degradation in African woodlands and forests. However, we caution against extrapolating this change in AGB to emissions, because, firstly, it is likely that many of the areas that are degraded are subsequently deforested (Ahrends *et al.*, 2010), and secondly, the time period over which a change in standing stocks translates into a flux to the atmosphere is currently unknown in this ecosystem.

Loss of AGB in our study area (0.43 MgC ha^{-1} yr^{-1}) was lower than has been reported from plot data in the surrounds of Dar es Salaam (0.8 MgC ha^{-1} yr^{-1}(Ahrends *et al.*, 2010)). This is expected given that our study site is ~100 km by road from the nearest city,Chimoio, which has a much smaller population and thus pressure for resource extraction is likely to be lower.

The distinction between deforestation and degradation is logical in the context of the area multiplied byC density approach to C stock estimation. However,the advent of high resolution maps of C stocks and their change, where the resolution is similar to the area of a single tree

canopy, means that the distinction becomes ambiguous – in effect degradation is just very small scale deforestation. It may be more useful to characterise a land cover change regime in terms of the frequency, area (and shape), and intensity of biomass change, as these parameters might be more easily related to the extent of different land uses, which is normally the information policy makers require.

- Are areas of high carbon density preferentially targeted for land cover change?

The difference between the AGB of land that underwent LCC and the mean of comparable surrounding woodland was <1 MgC ha^{-1}, suggesting there is no substantial preference for LCC to be undertaken in high biomass areas (Fig 7). There are some indications that this may not be true in all areas (such as Vunduzi), but for now, the hypothesis that emissions might be substantially higher as a result of preferential deforestation of high AGB areas has not been supported. This suggests that the other criteria for the location of new farms dominate (such as proximity to existing farms, roads or dwellings) or that AGB is not correlated to the agricultural suitability of the land. The latter might be true even if *potential* AGB and soil fertility are correlated because of past land use or other disturbance to AGB.

- What is the carbon density (MgC ha^{-1}) of changed areas before and after land cover change?

After a change event, land was not reduced to zero AGB, but instead averaged 11.9±18.4 MgC ha^{-1}. This result fits with observations on the ground, where large trees are often left in newly cleared areas to provide shade, or because of the disproportionate effort needed to remove them(Ghee, 2009). In addition, trees on deforested land are often ringbarked or otherwise killed, but left standing, and as they dry out will scatter radar waves less as their dielectric properties change. However, there is evidence ofnon-linearity in the AGB-backscatter regression at low values of backscatter, so these measurements of very low AGB values may be subject to additional uncertainties. This may be because at very low

biomass,backscatter will be strongly influenced by the properties of the ground surface, including surface roughness and soil moisture.

- What size are land cover change events, and how are they clustered in space?

In Central Mozambique, farmers have an arable area of 1.4 ha on average (Simler *et al.*, 2004). However, most LCC events detected in this study were much smaller than this (mean 0.45 ha), indicating that farms are built up in size by repeated small clearances (Fig 6). The significant spatial clustering of LCC events supports this. This 'death by a thousand cuts' type of woodland clearance poses a stiff challenge for rapid monitoring of LCC: A detection system that ignored events < 1 ha would miss the areal majority of LCC in this study area, and so might need to operate over long time scales to be effective.

Limitations

Despite only using dry season imagery, there is considerable variation through time in the backscattervalues of the ALOS PALSAR imagery, and the slope of the backscatter-AGB regression. This is presumably due to variations in environmental conditions such as soil moisture, which is well known to influence L-band backscatter(Rignot *et al.*, 1994, Pulliainen *et al.*, 1999, Magnusson *et al.*, 2007, Pantze *et al.*, 2009, Lucas *et al.*, 2010),changes to understory vegetation,or sensor calibration drift. This variation suggests that accurate biomass change detection with this sensor will require either: invariant features to be present in each scene; correction for e.g. the effects of soil moisture with ancillary data sets and models; or recalibration to ground data at each time point. We adopted the latter approach here, but with an inventory that was not repeated each year, and thus an assumption that plot biomass has not changed during the study period.

Furthermore, there are potentially significant uncertainties associated with the stem diameter-biomass allometry (Chave *et al.*, 2004) even with the use of a site-specific model. This can introduce bias of ~17% (Ryan, 2009). Although the regression procedure used here accounts

for the random error, the bias will remain and influence estimates of AGB stocks, but not change.

It should also be noted that the L-band biomass-backscatter response is known to saturate at the level of biomass typically found in closed canopy forests. Studies report saturation at between 30-100 MgC ha^{-1}(Mitchard *et al.*, 2009, Lucas *et al.*, 2010), although this appears to depend on vegetation structure (Lucas *et al.*, 2010). Thus the method presented here which utilises L-bandwill be most useful in low C density woodlands rather than higher density forests. The proposed BIOMASS mission would employ P-band radar in an effort to overcome this limitation (Le Toan *et al.*).

Conclusions

- Multi-temporal L-band radar imagery can be effective in detecting small-scale deforestation, but may fail to detect small levels of degradation over large areas. Abrupt changes of more than 12 MgC ha^{-1} are detectable at 95% confidence on a 25x25 m pixel scale.
- In this area of Mozambique, land cover change events are mostly small (median = 0.2 ha) but range from 0.06-18 ha and reduce aboveground carbon from 33.5 to 11.9 MgC ha^{-1} on average. They are strongly clustered together, and many events are the expansion of previously cleared land.
- There was no evidence that the areas that were deforested had a higher biomass than the average surrounding woodland.
- Degradation losses are likely to be substantial, with a best guess that they represent 67% of the netbiomass loss. This number is extremely uncertain however.

Acknowledgements

The Nhambita communityand staff of Envirotrade facilitated fieldwork. Staff of the Gorongosa national park allowed access to plots within the park. The GeoEye Foundation provided the IKONOS image. ESA and JAXA provided the ALOS imagery (C1P.7493).CRwas supported by the UK NERC Carbon Fusion project, the Mpingo Conservation & Development Initiative (http://tinyurl.com/mpingo) under their REDD Pilot Project funded by the Royal Norwegian Embassy in Tanzania, and the EU FP7 iREDD+ project.EM is funded by Gatsby Plants. We also thank Iain Cameron for his advice and help. We thank the two anonymous reviewers for their helpful comments.

References

Achard F., Defries R., Eva H. *et al.* (2007) Pan-tropical monitoring of deforestation. *Environmental Research Letters,***2**.

Ahrends A., Burgess N. D., Milledge S. a. H. *et al.* (2010) Predictable waves of sequential forest degradation and biodiversity loss spreading from an African city. *Proceedings of the National Academy of Sciences,***107**, 14556-14561.

Almeida-Filho R., Rosenqvist A., Shimabukuro Y. E. *et al.* (2005) Evaluation and perspectives of using multitemporal L-band SAR data to monitor deforestation in the Brazilian Amazoˆnia. *Geoscience and Remote Sensing Letters, IEEE,***2**, 409-412.

Archibald S., Scholes R. J. (2007) Leaf green-up in a semi-arid African savanna separating tree and grass responses to environmental cues. *Journal of Vegetation Science,***18**, 583-594.

Asf (2010) *ASF MapReady User Manual*, Alaska Satellite Facility Engineering Group.

Asner G. P., Powell G. V. N., Mascaro J. *et al.* (2010) High-resolution forest carbon stocks and emissions in the Amazon. *Proceedings of the National Academy of Sciences,***107**, 16738-16742.

Burgess N., Doggart N., Lovett J. C. (2002) The Uluguru Mountains of eastern Tanzania: the effect of forest loss on biodiversity. *Oryx,***36**, 140-152.

Chave J., Condit R., Aguilar S. *et al.* (2004) Error propagation and scaling for tropical forest biomass estimates. *Philosophical Transactions of the Royal Society of London Series B-Biological Sciences,***359**, 409-420.

Ciais P., Bombelli A., Williams M. *et al.* (in press) The carbon balance of Africa: synthesis of recent research studies. *Philosophical Transactions of the Royal Society (A),***369**, 1-20.

Defries R. S., Rudel T., Uriarte M. *et al.* (2010) Deforestation driven by urban population growth and agricultural trade in the twenty-first century. *Nature Geoscience,***3**, 178-181.

Denman K. L., Brasseur G., Chidthaisong A. *et al.* (2007) Couplings Between Changes in the Climate System and Biogeochemistry. In: *Climate Change 2007: The Physical Science Basis.* (eds Solomon S, Qin D, Manning M, Chen Z, Marquis M, Averyt KB, M.Tignor, Miller HL) pp Page. Cambridge, Cambridge University Press.

Dewees P. A., Campbell B. M., Katerere Y. *et al.* (2010) Managing the Miombo Woodlands of Southern Africa: Policies, Incentives and Options for the Rural Poor. *Journal of Natural Resources Policy Research,***2**, 57-73.

Etter A., Mcalpine C., Phinn S. *et al.* (2006) Characterizing a tropical deforestation wave: a dynamic spatial analysis of a deforestation hotspot in the Colombian Amazon. *Global Change Biology,***12**, 1409-1420.

Fao (2010) Global Forest Resources Assessment 2010. In: *FAO Forestry papers.* pp Page.

Farr T. G., Rosen P. A., Caro E. *et al.* (2007) The shuttle radar topography mission. *Reviews of Geophysics,***45**.

Fisher B. (2010) African exception to drivers of deforestation. *Nature Geosci,***3**, 375-376.

Fransson J. E. S., Magnusson M., Olsson H. *et al.* (2007) Detection of forest changes using ALOS PALSAR satellite images. In: *Geoscience and Remote Sensing Symposium, 2007. IGARSS 2007. IEEE International.* pp Page.

Frost P. (1996) The ecology of Miombo woodlands. In: *The Miombo in transition : woodlands and welfare in Africa.* (ed Campbell BM) pp Page. Bogor, Indonesia, Center for International Forestry Research.

Furley P. A., Rees R. M., Ryan C. M. *et al.* (2008) Savanna burning and the assessment of long-term fire experiments with particular reference to Zimbabwe. *Progress In Physical Geography,***32**, 611-634.

Geist H. J., Lambin E. F. (2002) Proximate Causes and Underlying Driving Forces of Tropical Deforestation. *BioScience,***52**, 143-150.

Ghee C. (2009) Nitrogen and Carbon Dynamics in Mozambican Smallholder Agroforestry Systems. MSc, University of Edinburgh, Edinburgh.

Gofc-Gold (2010) A sourcebook of methods and procedures for monitoring and reporting anthropogenic greenhouse gas emissions and removals caused by deforestation, gains and losses of carbon stocks in forests remaining forests, and forestation. pp Page, Alberta, GOFC-GOLD Project Office.

Grainger A. (1999) Constraints on modelling the deforestation and degradation of tropical open woodlands. *Global Ecology and Biogeography,***8**, 179-190.

Grainger A. (2008) Difficulties in tracking the long-term global trend in tropical forest area. *Proceedings of the National Academy of Sciences,***105**, 818-823.

Hansen M. C., Shimabukuro Y. E., Potapov P. *et al.* (2008) Comparing annual MODIS and PRODES forest cover change data for advancing monitoring of Brazilian forest cover. *Remote Sensing of Environment,***112**, 3784-3793.

Hoekman D. H., Vissers M. a. M., Wielaard N. (2010) PALSAR Wide-Area Mapping of Borneo: Methodology and Map Validation. *Selected Topics in Applied Earth Observations and Remote Sensing, IEEE Journal of,***3**, 605-617.

Houghton R. A. (2010) How well do we know the flux of CO2 from land-use change? *Tellus B,***62**, 337-351.

Houghton R. A., Hackler J. L. (2006) Emissions of carbon from land use change in sub-Saharan Africa. *Journal of Geophysical Research - Atmospheres,***111**.

Houghton R. A., Hall F., Goetz S. J. (2009) Importance of biomass in the global carbon cycle. *Journal of Geophysical Research-Biogeosciences,***114**.

Hui D., Jackson R. B. (2007) Uncertainty in allometric exponent estimation: A case study in scaling metabolic rate with body mass. *Journal of Theoretical Biology,***249**, 168-177.

Ine (2010) Estatísticas do Distrito de Gorongosa. pp Page, Instituto Nacional de Estatística.

Karjalainen M., Pyysalo U., Karila K. *et al.* (2009) Forest biomass estimation using ALOS PALSAR images in challenging natural forest area in Finland. In: *ALOS PI 2008 Symposium.* pp Page, Island of Rhodes, Greece, ESA Special Publication SP-664.

Kindermann G. E., Mcallum I., Fritz S. *et al.* (2008) A global forest growing stock, biomass and carbon map based on FAO statistics. *Silva Fennica,***42**, 387-396.

Le Toan T., Beaudoin A., Riom J. *et al.* (1992) Relating forest biomass to SAR data. *Geoscience and Remote Sensing, IEEE Transactions on,***30**, 403-411.

Le Toan T., Quegan S., Davidson M. W. J. *et al.* The BIOMASS mission: Mapping global forest biomass to better understand the terrestrial carbon cycle. *Remote Sensing of Environment,***In Press, Corrected Proof**.

Loarie S. R., Asner G. P., Field C. B. (2009) Boosted carbon emissions from Amazon deforestation. *Geophysical Research Letters,***36**.

Lucas R., Armston J., Fairfax R. *et al.* (2010) An Evaluation of the ALOS PALSAR L-Band Backscatter–Above Ground Biomass Relationship Queensland, Australia: Impacts of Surface Moisture Condition and Vegetation Structure. *Selected Topics in Applied Earth Observations and Remote Sensing, IEEE Journal of,***3**, 576-593.

Magnusson M., Fransson J. E. S., Eriksson L. E. B. *et al.* (2007) Estimation of forest stem volume using ALOS PALSAR satellite images. In: *Geoscience and Remote Sensing Symposium, 2007. IGARSS 2007. IEEE International.* pp Page.

Mayaux P., Bartholom, Etienne *et al.* (2004) A new land-cover map of Africa for the year 2000. *Journal Of Biogeography,***31**, 861-877.

Mertz O. (2009) Trends in shifting cultivation and the REDD mechanism. *Current Opinion in Environmental Sustainability,***1**, 156-160.

Miettinen J., Shi C., Liew S. C. (2011) Deforestation rates in insular Southeast Asia between 2000 and 2010. *Global Change Biology*, no-no.

Mitchard E. T. A., Saatchi S. S., Woodhouse I. H. *et al.* (2009) Using satellite radar backscatter to predict above-ground woody biomass: A consistent relationship across four different African landscapes. *Geophys. Res. Lett.,***36**, L23401.

Nepstad D. C., Verssimo A., Alencar A. *et al.* (1999) Large-scale impoverishment of Amazonian forests by logging and fire. *Nature,***398**, 505-508.

Pantze A., Krantz A. H., Fransson J. E. S. *et al.* (2009) Mapping and monitoring clear-cuts in Swedish forest using ALOS PALSAR satellite images. In: *Geoscience and Remote Sensing Symposium,2009 IEEE International,IGARSS 2009.* pp Page.

Pulliainen J. T., Kurvonen L., Hallikainen M. T. (1999) Multitemporal behavior of L- and C-band SAR observations of boreal forests. *Geoscience and Remote Sensing, IEEE Transactions on,***37**, 927-937.

Radke R. J., Andra S., Al-Kofahi O. *et al.* (2005) Image change detection algorithms: a systematic survey. *Image Processing, IEEE Transactions on,***14**, 294-307.

Rahman M., Sumantyo J. (2010) Mapping tropical forest cover and deforestation using synthetic aperture radar (SAR) images. *Applied Geomatics,***2**, 113-121.

Ramankutty N., Gibbs H. K., Achard F. *et al.* (2007) Challenges to estimating carbon emissions from tropical deforestation. *Global Change Biology,***13**, 51-66.

Rignot E., Way J., Williams C. *et al.* (1994) Radar estimates of aboveground biomass in boreal forests of interior Alaska. *Geoscience and Remote Sensing, IEEE Transactions on,***32**, 1117-1124.

Rignot E. J. M., Van Zyl J. J. (1993) Change detection techniques for ERS-1 SAR data. *Geoscience and Remote Sensing, IEEE Transactions on,***31**, 896-906.

Ryan C. M. (2009) Carbon Cycling, Fire and Phenology in a Tropical Savanna Woodland in Nhambita, Mozambique. PhD, University of Edinburgh, Edinburgh, 257 pp.

Ryan C. M., Williams M. (2011) How does fire intensity and frequency affect miombo woodland tree populations and biomass? *Ecological Applications,***21**, 48-60.

Ryan C. M., Williams M., Grace J. (2011) Above- and Belowground Carbon Stocks in a Miombo Woodland Landscape of Mozambique. *Biotropica*.

Schmidt-Vogt D., Leisz S., Mertz O. *et al.* (2009) An Assessment of Trends in the Extent of Swidden in Southeast Asia. *Human Ecology,***37**, 269-280.
Shimada M., Tadono T., Rosenqvist A. (2010) Advanced Land Observing Satellite (ALOS) and Monitoring Global Environmental Change. *Proceedings of the IEEE,***98**, 780-799.
Simler K. R., Mukherjee S., Dava G. L. *et al.* (2004) Rebuilding after War: Micro-level Determinants of Poverty Reduction in Mozambique. pp Page, Washington DC, International Food Policy Research Institute.
Sokal R. R., Rohlf F. J. (1995) *Biometry : the principles and practice of statistics in biological research,* New York, W.H. Freeman.
690 Tinley K. L. (1977) Framework of the Gorongosa Ecosystem. D.SC, University of Pretoria, Pretoria, 184 pp.
Tinley K. L. (1982) The influence of soil moisture balance on ecosystem patterns in Southern Africa. In: *Ecology of tropical savannas.* (eds Huntley BJ, Walker BH) pp Page. Berlin, Springer.
Trujillo-Ortiz A., Hernandez-Walls R. (2010) Geometric Mean Regression (Reduced Major Axis Regression). pp Page.
Van Der Sanden J. J., Hoekman D. H. (1999) Potential of Airborne Radar To Support the Assessment of Land Cover in a Tropical Rain Forest Environment. *Remote Sensing of Environment,***68**, 26-40.
Van Der Werf G. R., Morton D. C., Defries R. S. *et al.* (2009) CO2 emissions from forest loss. *Nature Geosci,***2**, 737-738.
Williams C., Hanan N., Neff J. *et al.* (2007) Africa and the global carbon cycle. *Carbon Balance and*
700 *Management,***2**, 3.
Williams M., Ryan C. M., Rees R. M. *et al.* (2008) Carbon sequestration and biodiversity of re-growing miombo woodlands in Mozambique. *Forest Ecology And Management,***254**, 145-155.
Woodhouse I. H. (2006a) *Introduction to microwave remote sensing,* New York ; London, Taylor & Francis.
Woodhouse I. H. (2006b) Predicting backscatter-biomass and height-biomass trends using a macroecology model. *Geoscience and Remote Sensing, IEEE Transactions on,***44**, 871-877.

Figures and Tables

Table 1. Regression statistics for the relationship betweenradar backscatter (unitless) and aboveground woody biomass (MgC ha^{-1}). RMA indicates reduced major axis regression. OLS ordinary least squares regression.

Date	RMA Slope(MgC ha^{-1})$^{-1}$		RMA Intercept (MgC ha^{-1})		OLS	Calibration error	Validation error	Validation bias
	Slope	95% confidence interval	Intercept	95% confidence interval	adj R^2	RMSE (MgC ha^{-1})	RMSE (MgC ha^{-1})	Bias (MgC ha^{-1})
23-Jun-07	1562	1315–1810	-20.9	-26.6–-15.1	0.39	10.4	10.9	1.7
08-Aug-07	1268	1082–1453	-13.7	-18.0–-9.5	0.49	9.3	9.9	1.5
23-Sep-07	1329	1153–1505	-11.0	-14.5–-7.5	0.58	8.4	8.7	1.4
10-May-08	1647	1417–1877	-22.6	-27.9–-17.3	0.53	8.9	9.3	1.5
25-Jun-08	1632	1385–1880	-19.9	-25.2–-14.5	0.44	9.8	10.4	1.6
28-Jun-09	1601	1363–1840	-17.5	-22.3–-12.6	0.47	9.6	10.1	1.6
28-Sep-09	1303	1115–1490	-11.2	-15.0–-7.4	0.50	9.2	9.6	1.5
16-May-10	1801	1518–2083	-24.7	-31.0–-18.4	0.41	10.3	10.7	1.7
01-Jul-10	1679	1431–1926	-25.6	-31.6–-19.6	0.48	9.5	9.9	1.6
01-Oct-10	1348	1169–1526	-13.3	-17.0–-9.5	0.58	8.4	8.7	1.4
mean	*1517*	*1295–1739*	*-18.0*	*-22.9–-13.1*	*0.49*	*9.4*	*9.8*	*1.6*

Table 2. Change in aboveground biomass (AGB) stocks classified by forest/non-forest transitions over the period 2007-2010. The threshold for forest is AGB>15MgC ha^{-1}. Negative changes indicate a gain in biomass stocks.

Transition type	**Area (km^2)**	**AGB loss over three years (GgC)**	
Deforestation (forest→ non-forest)	75	92±11	55±12 (33%)
Aggradation (non-forest→ forest)	48	-36±4.5	
Forest degradation (forest→forest)	530	42 ±73	94±90 (67%)
Non-forest degradation (non-forest→non-forest)	507	53±43	
All	1160	149±101	

Figure1.Estimated carbon stocks in the study area in a) 2007 and b) 2010. Each image is derived from themean of three ALOS PALSAR scenes from that year's dry season. c) shows the areas detected as undergoing abrupt change (red) with a probability greater than 95% and a reduction in biomass to less than 50% of original biomass. Areas that did not undergo change are indicated in grey, and white indicates areas with < 10tC/ha. The maps are annotated with the local road network and the "sub-areas" used in Fig 7. (GIS data courtesy of ARA-CENTRO).

Figure 2. Histogram of the aboveground biomass(AGB) of the plots used to estimate and validate the AGB-backscatter relationship. Aboveground woody carbon stock is estimated from DBH measurements using a site-specific allometric equation.n = 96.

Figure 3.Regression of radar backscatterfrom ALOS PALSAR and aboveground biomass. Ten regressions were performed, one for each image in Table 1, but for clarity only the data and regression lines from the first (June-2007, open circle, dashed line), sixth (June-2009, closed circles, light line) and last (Oct-2010, crosses, heavy line) image are shown. Each line is fit to minimise the errors on both axes (RMA regression).

Figure4. Example time series fora single pixel over a) an undisturbed riverine forest (solid line, filled circles) and b) an area of woodland converted to a farm (dashed line, open circles). The lines indicate the parameters as estimated by the change detection algorithm. Over the protected forest no change was detected (mean AGB of 55.0±4.5 MgC ha^{-1}). The new farm (illustrated in Fig 6) was created between June 2008 and June 2009. AGB before the change point was 42.7±1.8 and 5.3±5.3 MgC ha^{-1}afterwards. The probability of this change being observed by chance is < 0.001. The points representing the forest pixel have been shifted forward by 10 days for clarity.

Figure 5. Carbon stock change in the study area. The image shows the aboveground biomass (AGB)in 2010 as a percentage of AGB in 2007. Values greater than 100% indicate areas of biomass gain(blue)and below 100% areas of biomass loss (red). Features lettered A-F aredescribed in the main text. Areas with AGB <10 tC are shown in white. The red box indicates the area shown in Fig 6. The red line shows the EN1 highway. Rivers are marked in blue.

Figure 6. Detail of Fig 5, showing the detected land cover change events. The temporal evolution of forest clearance as detected by the radar imagery is shown from 2007 to 2010 (left panels). The right hand panels show false-colour optical imagery of the same area for comparison. The outlines of the change events up to July 2009 are overlaid on the middle right image.

Figure7.Probability density functions of aboveground biomass in 2007 (black solid line), 2010 (grey solid line). Also shown is the AGB of changed pixels prior to change (dashed lines). The observed values (grey dashed lines), and the expected value if deforestation was random with respect to biomass (black dashed line) are shown. The 2007 and 2010 data are the mean of three images. The boundaries of each sub-area (a-g) are shown in Fig 1. No data are shown for the changed pixels in the Sanctuary as the number of changed pixels (n=10) was to few to produce a meaningful PDF.

Figure8. Miss rates and false positives for the land cover change detection algorithm under a variety of definitions of change. The P-value shown on the x axis are the threshold probability above which a change event is considered real. The various lines indicate φ, the fraction of biomass remaining after change, below which the pixel's biomass needs to be reduced for the change to be detected. A P-value of 0.95 and φ = 50% were used as default values.

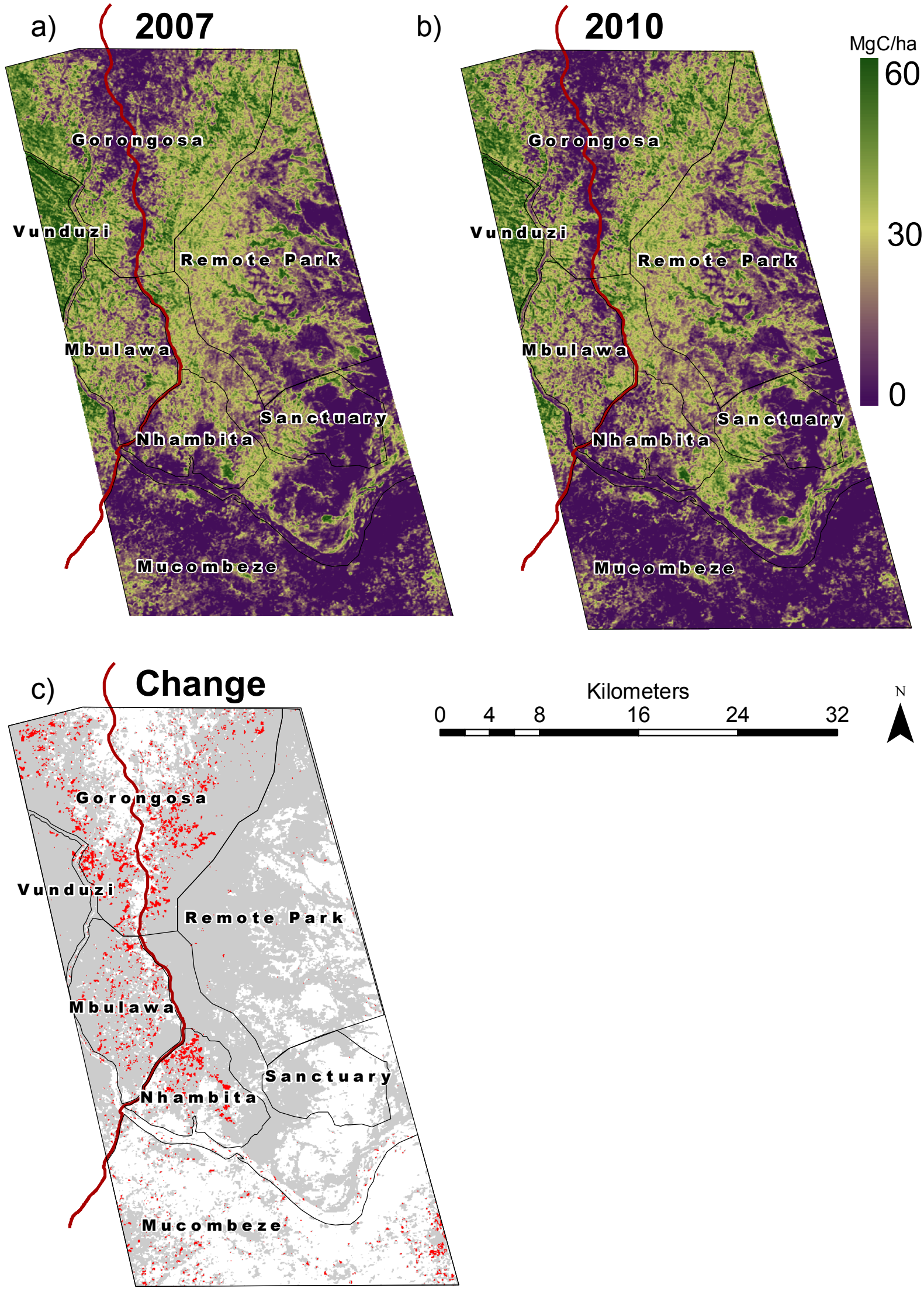
a)
2007
b)
2010
MgC/ha
60
30
0
Gorongosa
Vunduzi
Remote Park
Mbulawa
Sanctuary
Nhambita
Mucombeze
c)
Change
Kilometers
0 4 8 16 24 32
N

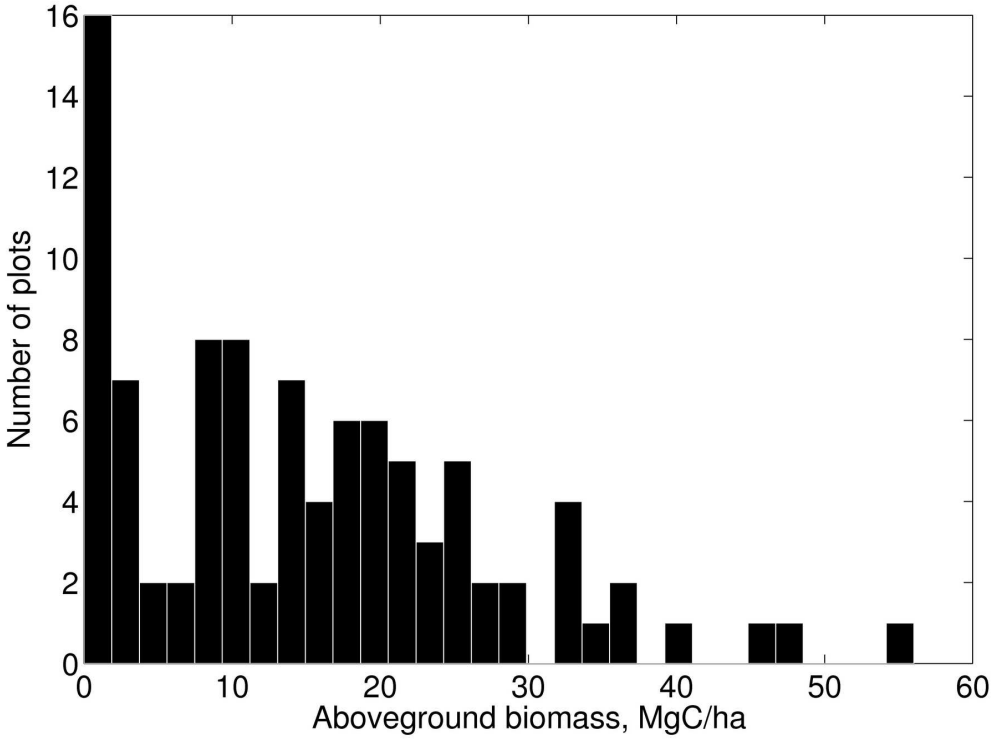

152x114mm (300 x 300 DPI)

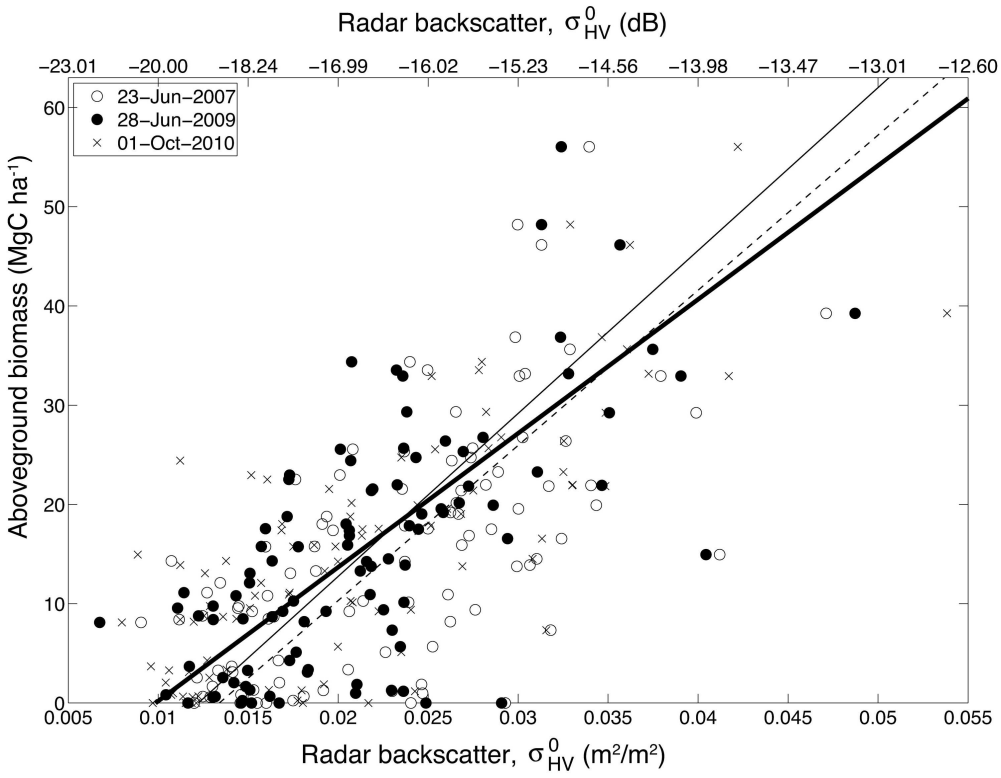

255x198mm (300 x 300 DPI)

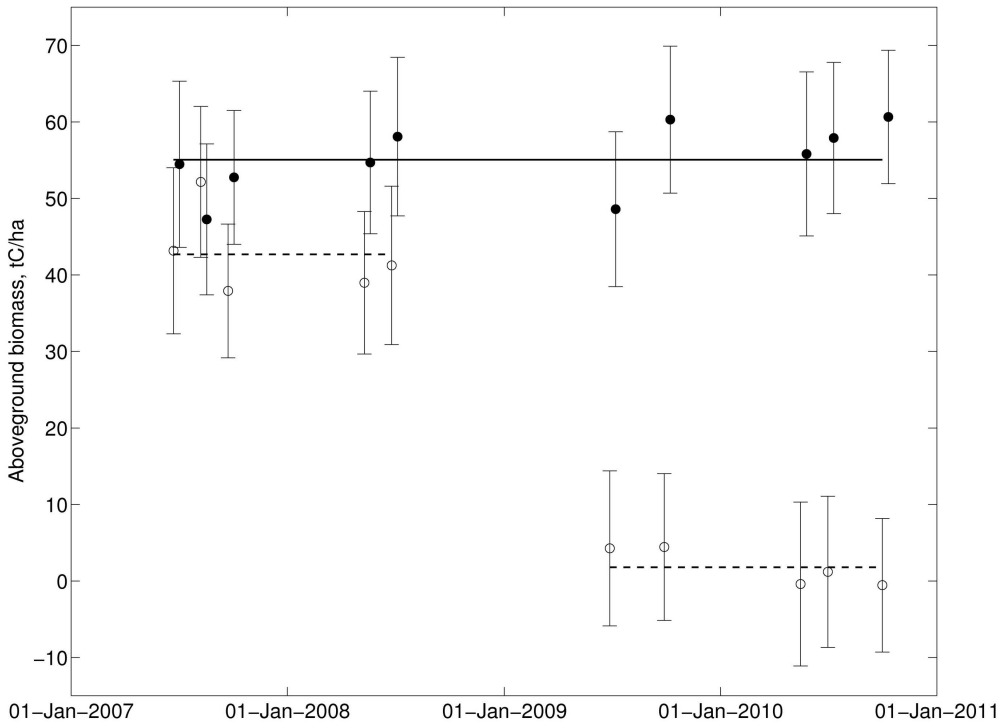

233x174mm (300 x 300 DPI)

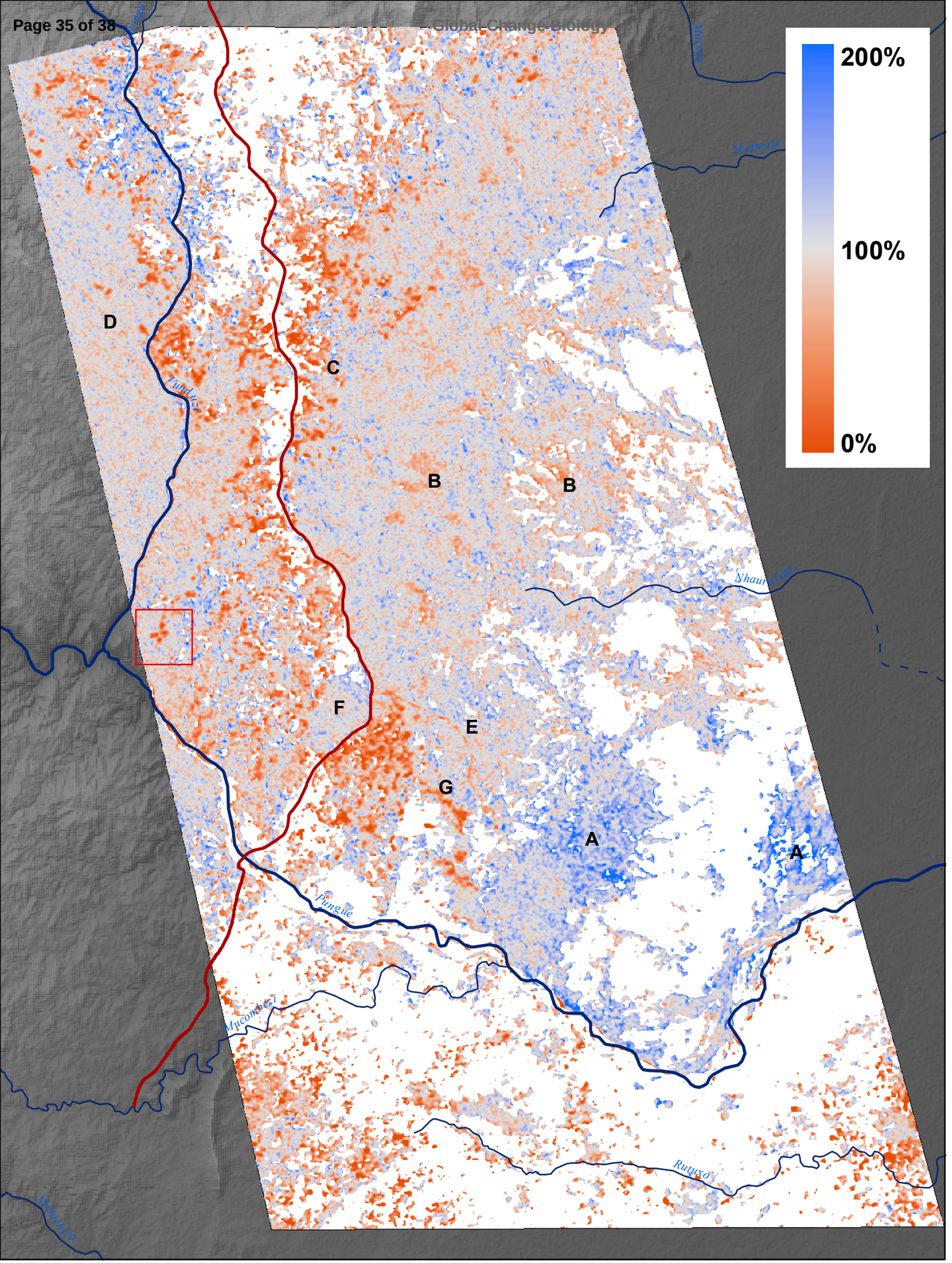

N

0 3 6 12 18 24 Kilometers

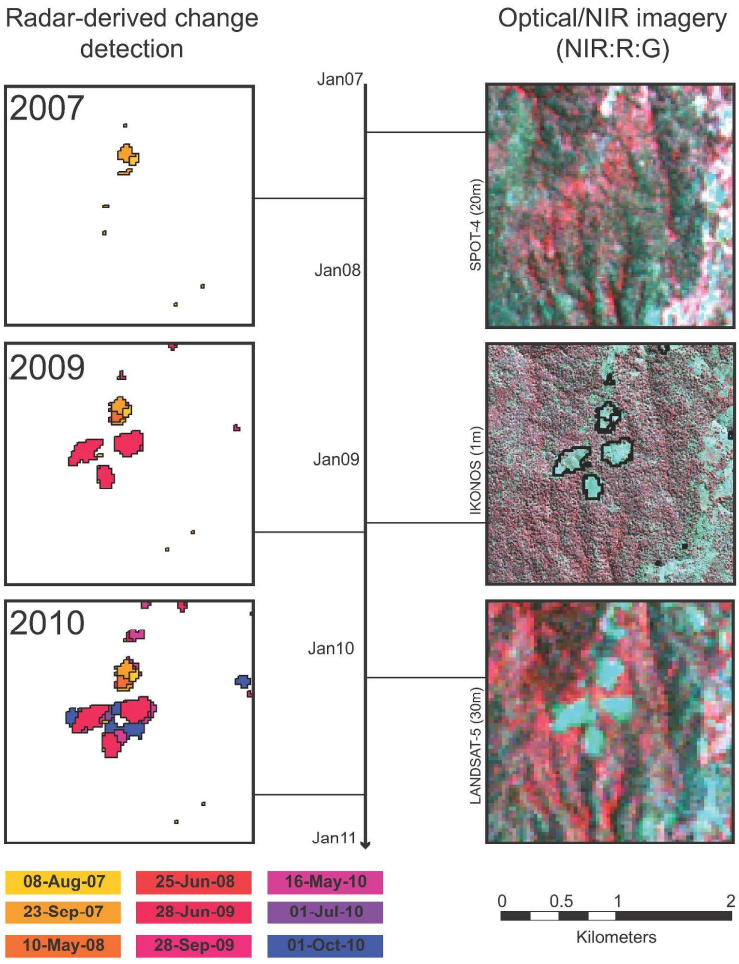

297x420mm (300 x 300 DPI)

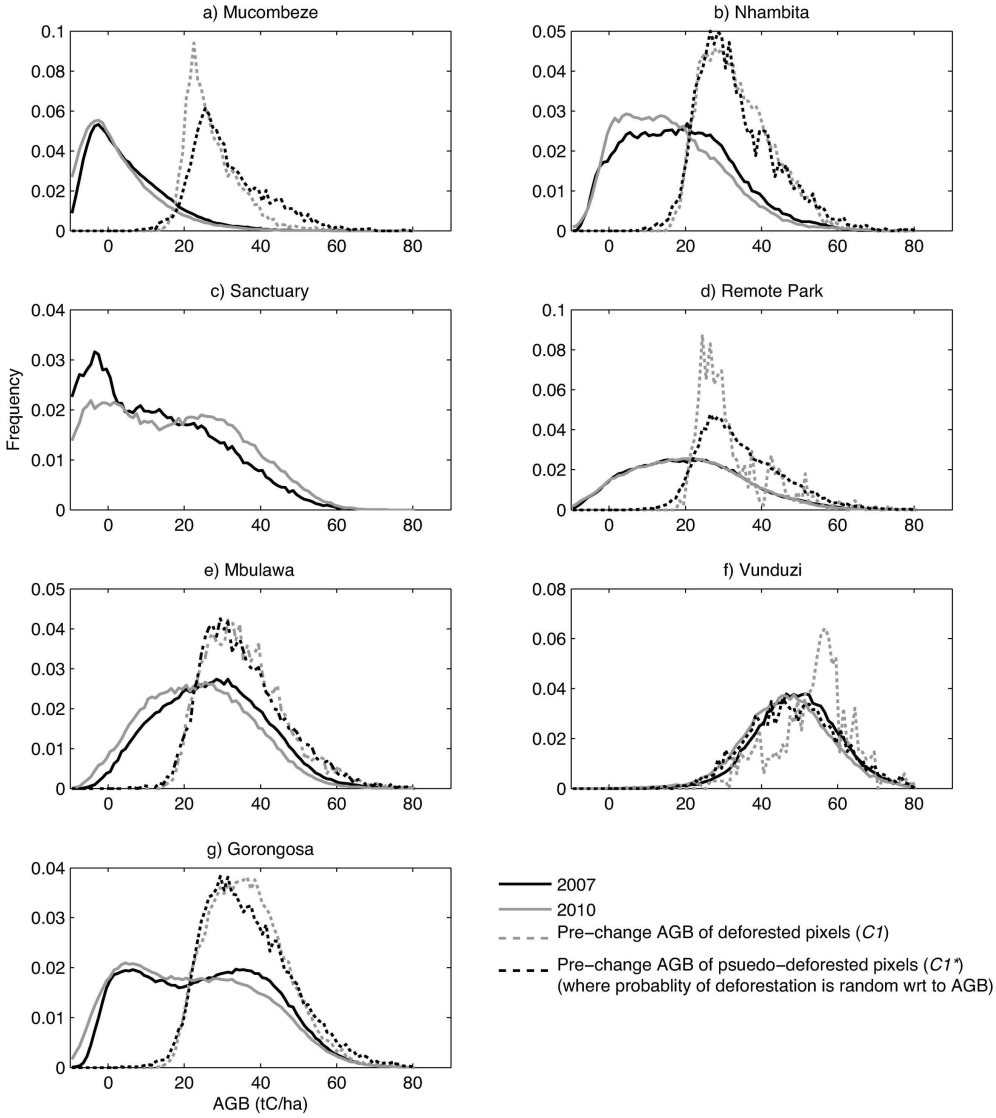

224x250mm (300 x 300 DPI)

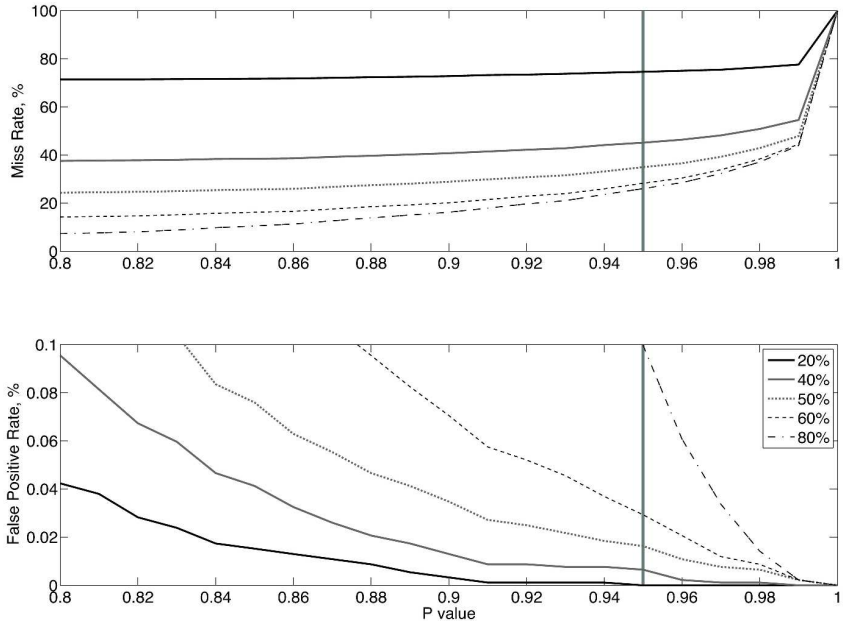

278x195mm (300 x 300 DPI)